ELSEVIER

Chemical Engineering Journal 67 (1997) 115–121

Chemical Engineering Journal

Kinetics of wet air oxidation of phenol

J.R. Portela Miguélez, J. López Bernal, E. Nebot Sanz, E. Martínez de la Ossa *

Department of Chemical Engineering, Food Technology and Environmental Technologies, Faculty of Sciences, University of Cádiz, 11510 Puerto Real, Cádiz, Spain

Received 8 August 1996; revised 3 January 1997; accepted 3 March 1997

Abstract

Aqueous solutions of phenol were oxidized in a batch reactor at temperatures between 150 and 300 °C and pressures from 100 to 200 bar. The initial phenol concentrations were between 460 and 1650 ppm and the initial oxygen concentration was always above 800% excess. The oxidation experiments covered essentially the entire range of phenol conversions and included all temperature ranges studied by previous workers. The reduction of COD during oxidation was also measured. Furthermore, pyrolysis experiments were carried out to verify that phenol is not degraded by this mechanism in the conditions studied.

Due to disagreement in the previous published data about the activation energy, an effort has been made to obtain reliable kinetic data, assuring great oxygen excess and minimum disturbance in the sampling procedure. The oxidation reaction was found to be pseudo-first order with respect to phenol, with an activation energy of 34.4 kJ mol^{-1}. The influence of pressure and temperature on the induction time was also studied. © 1997 Elsevier Science S.A.

Keywords: Kinetics; Wet air oxidation; Phenol; Pseudo first order; Induction time

1. Introduction

The effective removal of organic pollutants from industrial wastewater is a problem of great importance, due to their potentially harmful effects and the need to meet stringent statutory regulations. Effective treatment technologies which accomplish the destruction of these wastes into innocuous end products need to be established. Phenol and substituted phenols are commonly present in industrial waste streams, even in concentrations of 15 000 ppm [1], and are priority pollutants as they are extremely toxic, even in the parts per billion range [2].

Wet air oxidation (WAO), first developed and applied as a commercial process by Zimmerman and Diddams [3,4], is an effective destruction method for the treatment of hazardous organic wastes, especially when these are too dilute to incinerate and too toxic to biotreat [5,6]. WAO is a process by which components are oxidized in a liquid phase by oxygen that is provided by compressed air. The process takes place at elevated pressures, to enhance the solubility of oxygen in the aqueous solution and to keep water in the liquid state, and at elevated temperatures to make possible a rapid reaction. The oxidation products may be inorganic salts, simple forms of biodegradable compounds or may lead to complete oxidation to carbon dioxide and water [7,8].

Several authors have chosen phenol as a model component to gain kinetic data about the oxidation process [9–14]. It has been established that phenol wet oxidation follows a free radical mechanism and three reaction stages may be distinguished: an induction period in which there is very little or no measurable change in phenol concentration, a fast reaction phase in which the rate constant is far higher than that of the first stage, and a final stage, when most of phenol has been oxidized, in which the reaction rate constant is far lower than in the middle stage, and practically all the free radicals have been removed by a termination reaction.

However, the published literature on WAO of phenol is contradictory. Table 1 shows the values presented by several authors with respect to the activation energy (E_a) corresponding to the fast reaction phase.

The disagreement in published data can be explained in various ways. On the one hand, a variety of potential problems related to vapor–liquid equilibrium effects caused by sample withdrawal from the batch reactor may affect the raw concentration–time data [15].

On the other hand, as Devlin and Harris [16] proposed, the mechanism of the oxidation of aqueous phenol with dissolved oxygen varies as the ratio of phenol/oxygen goes from

---

* Corresponding author. Tel: +34 956 830907; fax: +34 956 837565.

1385-8947/97/$17.00 © 1997 Elsevier Science S.A. All rights reserved
PII S1385-8947(97)00025-9

Table 1
Summary of activation energies and reaction orders found by previous workers (corresponding to the fast reaction phase)

Temperature range (°C)	Phenol order	Oxygen order	Activation energy (kJ mol^{-1})	Reference
180–210	1	1	107	[9]
90–180	1	0.5	175	[10]
185–230	1	0–1	20	[12]
200–250	1	1	45	[11]
150–180	1	1	50	[14]
130–200	1	0.5	112	[13]

excess oxygen to excess phenol. So, under conditions of oxygen excess, intermediate ring compounds, dihydric phenols and quinones were not observed. In this way, Pruden and Le [11] proposed that shorter activation energies could be characteristic of total oxidation to carbon dioxide and water, while the greatest values are probably the result of polymerization reactions under conditions near the stoichiometric ratio of oxygen/phenol and under conditions of phenol excess. Moreover, the temperature range studied is always very reduced, not covering the whole subcritical wet oxidation range, and varying from author to author.

The aim of the study presented in this paper is to gain kinetic data regarding wet air oxidation of phenol at a wide range of temperatures and pressures which includes all previous studies in subcritical conditions, also assuring that there was a great oxygen excess in each experiment, giving only reactions of true oxidation. Moreover, a considerable effort to tune analytical methods for phenol analysis and sampling procedure has been made in this work. The influence of pressure and temperature on the induction time and on the final quality of the effluent have also been studied.

2. Experimental

2.1. Equipment

The experimental apparatus is sketched in Fig. 1. The reactor is a 316 stainless steel 300 ml autoclave manufactured by Autoclave Engineers, fitted with a variable speed "Magnedrive" stirrer and an electric furnace. The temperature controller (PID) held the temperature within ±2 °C of setpoint. The gas inlet, the injection system, pressure gauge and safety head port were situated on the top head. The injection system is a 0.25 inch O.D. tubing with on–off Swagelok valves, having a volume of 4 ml.

The sampling port for liquid samples consists of internal 0.125 inch O.D. tubing from the top head to the reactor bottom, connected through an on–off valve to an external 0.25 inch O.D. sampling tube with 4 ml volume. The internal sampling tube has a volume of 0.25 ml which affects the raw data. Before the first sample withdrawal, this tube contains only pure water because there is no mixture with the solution injected, so there is a dilution effect on the total volume sampled. In the following samples, this dead volume contains a solution with the previous sample composition. It is supposed that this liquid does not suffer oxidation due to the lack of oxygen inside the tube. In this way, the concentration effect that it produces on each sampling must be considered. The gas sampler consists of a 25 cm^3 volume glass vessel with a valve at each end.

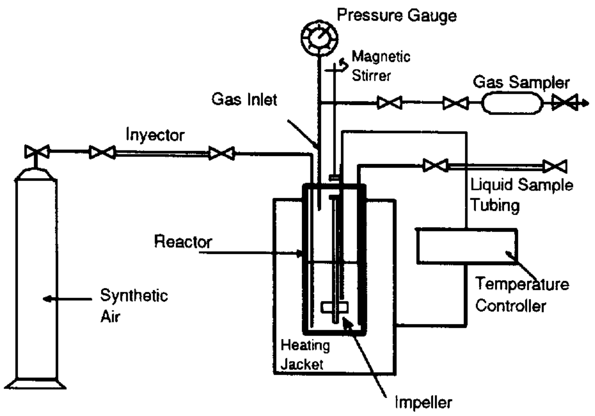

Fig. 1. Schematic diagram of the experimental wet air oxidation apparatus.

2.2. Procedure

The reactor was charged with 100 ml of deionized water and with a precalculated amount of synthetic air (Carburos Metálicos, 99.99% pure). The system was preheated up to the desired temperature for each experiment and the stirrer speed was adjusted to 10 rev/s^{-1}. Once the prefixed temperature was attained, a precalculated volume of phenol (Panreac, 99.5% pure) concentrated solution was injected into the autoclave by means of the pressure supplied by the bottled compressed air, therefore adjusting the experimental reaction pressure. The injection time was taken as the zero time for the reaction. Liquid samples were periodically withdrawn and analyzed until the concentration was less than 1% of its initial value. The reaction temperature and pressure were maintained during the course of the experiment. At the end of each experiment, when room temperature had been reached, gas effluent was depressurized slowly and passed through the gas sampler. A single gas sample was taken and analyzed by gas chromatography in order to determine the gas product composition and to verify that oxygen excess remained.

The same experimental procedure was followed for pyrolysis experiments but using N_2 (Carburos Metálicos, 99.99% pure) as the gas medium to avoid oxidation during each run.

2.3. Analytical methods

A Perkin–Elmer (Autosystem) gas cromatograph equipped with a flame ionization detector (FID) was used to analyze the phenol content, intermediate and final products such as organic acids. A 30 m length and 0.25 mm diameter capillary column Nukol (SUPELCO) was used, keeping the furnace temperature at 150 °C during 7 min for organic acid analysis and ramping at 30 °C min^{-1} to 180 °C for phenol determination.

A five-level calibration method with an external standard was used to calibrate the phenol analysis method, obtaining a correlation coefficient of 0.9988. A single level calibration method with an external standard of 0.1% of acetic, propionic, butyric, isobutyric, and valeric acids was used to calibrate volatile organic acid content.

Gas samples were analyzed on a Konic 2000 gas cromatograph with a thermal conductivity detector and a 2 m Carbosieves II (SUPELCO) packed column. A temperature ramp from 55 °C to 150 °C (at 30 °C min^{-1}) was used to separate the N_2/O_2 mixture from CO_2, and other possible gases (CO, NO_x). The system was calibrated with a standard gas mixture containing H_2, N_2, CO_2 and CH_4 supplied by Carburos Metálicos.

The method used for COD determination was adopted according to Standard Methods for the examination of water and wastewater [17].

3. Results and discussion

The overall oxidation process is controlled by two steps: (i) mass transfer of oxygen from the gas phase to the liquid phase; and (ii) reaction between the dissolved oxygen and phenol. As Joglekar et al. [14] demonstrated, the resistance of the first step can be eliminated by manipulating the speed of agitation. In our case it was found that the oxidation rate was speed independent when the speed of agitation was fixed at 10 rev s^{-1} or more. Some experiments were carried out at 20 rev s^{-1} obtaining similar results.

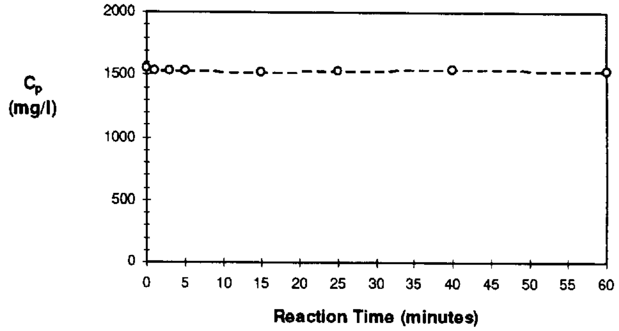

Fig. 2. Evolution of phenol concentration in the pyrolysis experiment at 300 °C.

Experimental conditions and initial values of phenol and oxygen concentrations of each experiment are presented in Table 2. As can be seen, oxygen was always in great excess in comparison to the stoichiometric oxygen concentration needed to complete the phenol oxidation to carbon dioxide and water.

None of the pyrolysis experiments showed any degradation of phenol in the conditions studied, so in the absence of oxygen, phenol is not thermally destroyed. Therefore, the main reaction taking place in the other experiments is the reaction of oxidation. Fig. 2 shows the result of the pyrolysis experiment under the most severe conditions. The data obtained in these experiments also shows that the sampling procedure does not produce a decrease in the concentration of the liquid, due to the minimum volume sampled and the correction of the raw concentration data regarding the dead volume in the internal sampling tube.

Figs. 3–5 show the variation of normalized phenol concentration (defined as the actual to initial phenol concentration ratio, C_P/C_{P_0}) versus time, during oxidation experiments at different pressures (100, 150 and 200 bar, respectively).

Table 2
Summary of experiments

Run	Pressure (bar)	Temp. (°C)	C_{P_0} (mol l^{-1}) $\times 10^3$	C_O (mol l^{-1})	Oxygen excess [a] (%)	k (min^{-1})	k Standard error
Pyrolysis							
1	150	200	17.522	0	–	–	–
2	150	250	17.543	0	–	–	–
3	150	300	16.576	0	–	–	–
Oxidation							
4	100	150	13.856	0.5832	950	–	–
5	100	200	11.922	0.5176	880	0.4497	0.034
6	100	250	8.458	0.4688	980	0.8676	0.046
7	100	300	4.888	0.4280	1230	0.9876	0.089
8	150	150	15.291	0.8603	1260	0.1299	0.014
9	150	200	16.916	0.7655	930	0.3882	0.074
10	150	250	11.848	0.6875	1050	0.9106	0.124
11	150	300	8.607	0.6270	1060	1.181	0.096
12	200	150	15.981	1.1198	1500	–	–
13	200	200	16.321	0.9988	1260	0.3916	0.030
14	200	250	16.055	0.8967	1000	0.9353	0.042
15	200	300	16.385	0.8165	750	1.4828	0.087

[a] Oxygen excess refers to the available oxygen in the reactor to stoichiometric oxygen ratio.

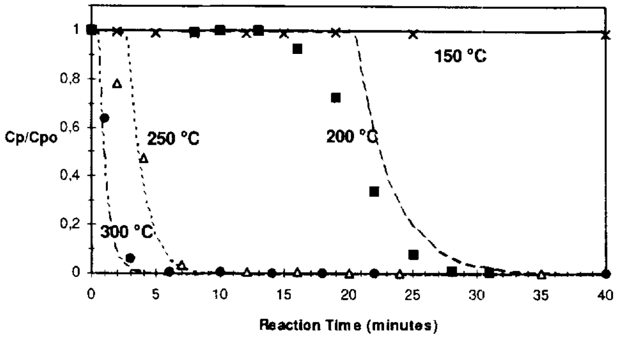

Fig. 3. Measured normalized phenol concentration plotted versus residence time for several temperatures at 100 bar. Symbols denote experimental data and lines denote prediction from the kinetic model, for run 4 (150 °C) ×———, run 5 (200 °C) ■– – –, run 6 (250 °C) △- - -, and run 6 (300 °C) ●– · · –.

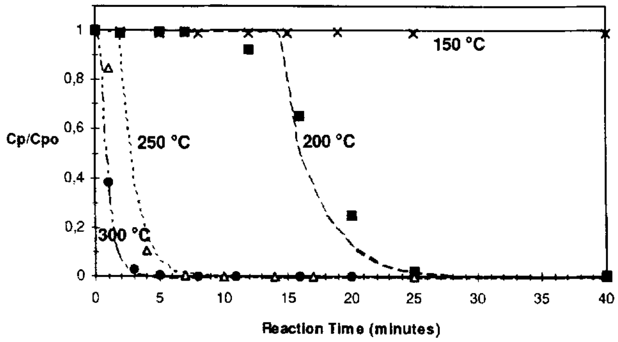

Fig. 4. Measured normalized phenol concentration plotted versus residence time for several temperatures at 150 bar. Symbols denote experimental data and lines denote prediction from the kinetic model, for run 8 (150 °C) ×———, run 9 (200 °C) ■– – –, run 10 (250 °C) △- - -, and run 11 (300 °C) ●– · · –.

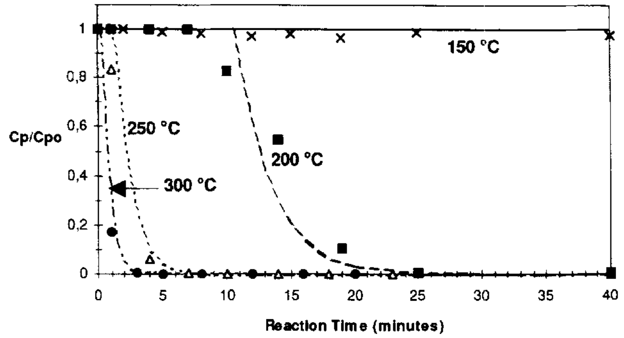

Fig. 5. Measured normalized phenol concentration plotted versus residence time for several temperatures at 200 bar. Symbols denote experimental data and lines denote prediction from the kinetic model, for run 12 (150 °C) ×———, run 13 (200 °C) ■– – –, run 14 (250 °C) △- - -, and run 15 (300 °C) ●– · · –.

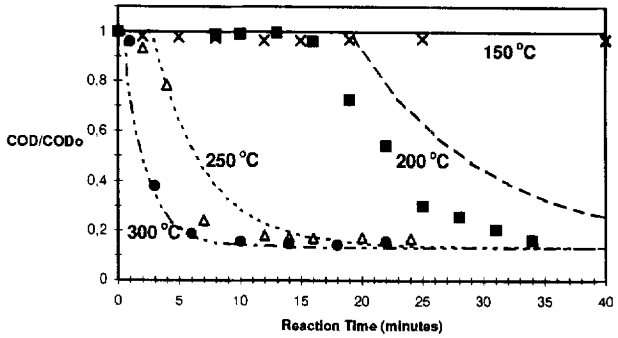

Fig. 6. Measured normalized COD concentration plotted versus reaction time for several temperatures at 100 bar. Symbols denote experimental data and lines denote prediction from the kinetic model, for runs run 4 (150 °C) ×———, run 5 (200 °C) ■– – –, run 6 (250 °C) △- - -, and run 6 (300 °C) ●– · · –.

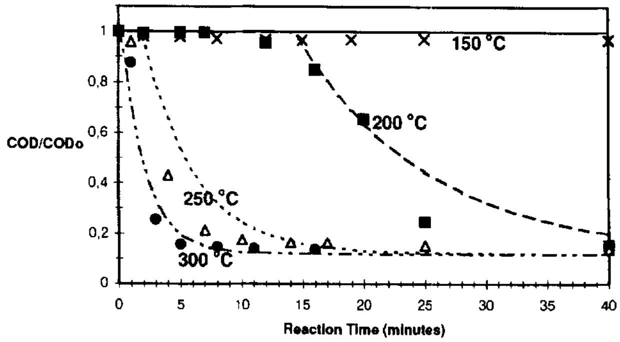

Fig. 7. Measured normalized COD concentration plotted versus reaction time for several temperatures at 150 bar. Symbols denote experimental data and lines denote prediction from the kinetic model, for run 8 (150 °C) ×———, run 9 (200 °C) ■– – –, run 10 (250 °C) △- - -, and run 11 (300 °C) ●– · · –.

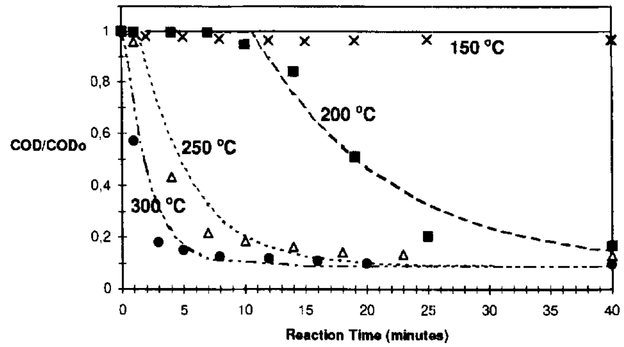

Fig. 8. Measured normalized COD concentration plotted versus residence time for several temperatures at 200 bar. Symbols denote experimental data and lines denote prediction from the kinetic model, for run 12 (150 °C) ×———, run 13 (200 °C) ■– – –, run 14 (250 °C) △- - -, and run 15 (300 °C) ●– · · –.

In these figures the three reaction steps, induction, fast oxidation and termination can be clearly distinguished. The induction time, which was over 1 h at 150 °C, decreases as the temperature rises, until it almost disappears at 300 °C. On the other hand, in the oxidation period, it can be seen that the phenol disappearance rate increases with increasing temperature.

A similar study can be carried out for COD/COD$_0$ versus temperature, as shown in Fig. 6–8. The results obtained show a similar trend, though a lower elimination grade is observed in every case, due to the persistence of intermediate oxidation products, like acetic, propionic, butiric and other organic acids that are refractory to wet air oxidation. Therefore, major deviations for the greatest values of conversion were obtained between experimental data and predictions from the kinetic model that is proposed. The reason is that activation energy and pre-exponential have been calculated for the fast reaction period, in which phenol oxidation takes place, but not for organic acids, which produce a residual COD with a much higher activation energy. So, in these cases, deviations have been corrected by introducing a residual value of COD/COD_o, corresponding to the maximum elimination efficiency obtained at the highest temperature of each reaction pressure.

Despite the formation of refractory compounds, since these intermediate products are far less toxic than phenol, the toxicity removal is much larger than the COD removal. Moreover, simple organic acids are highly biodegradable, so, according to other authors, one of the most interesting prospects is the use of wet oxidation as pretreatment before a biological treatment [18]. On the other hand, it would be possible to completely oxidize the phenol content with total COD removal by working in more severe conditions, such as oxidation in supercritical water [19–22].

3.1. Reaction kinetics

The objectives of present kinetic analysis were to determine the reaction rate constant (k), its associated Arrhenius parameters, and the reaction order for phenol. According to a second-order irreversible reaction, the kinetic expression obtained by applying the integral method of kinetic data analysis [23] is given by the following equation:

$$\ln\frac{C_O C_{Po}}{C_{Oo} C_P} = (C_{Oo} - C_{Po})kt \quad (\text{for } C_{Oo} \neq C_{Po}) \tag{1}$$

where C_O is oxygen concentration, C_P is phenol concentration and subscript 'o' denotes initial concentration.

If the initial oxygen concentration is much greater than initial phenol concentration, the oxygen concentration can be considered practically invariable during the reaction, so it is possible to approximate the expression to pseudo-first order, given by the equation:

$$-\ln\frac{C_P}{C_{Po}} = kt \tag{2}$$

As shown in Table 2, in all the experiments initial oxygen concentration was fixed at a great excess over the stoichiometric concentration needed to oxidize phenol completely. Thus, the rate constant (k) can be calculated from the slope of the straight line obtained when ln (C_P/C_{Po}) is represented versus time in the period in which rapid oxidation occurs. Fig. 9 shows a typical result of the linear regression to experimental data. The intercept of the straight line with the abscissas corresponds to the induction time.

Following this procedure, k values were calculated for all temperature and pressure conditions studied. These values are presented in Table 2, showing that k increases with increasing temperature, but it is not significatively affected by reaction pressure between 100 and 200 bar.

Assuming that k has an Arrhenius behaviour, both the pre-exponential, k_o, and the activation energy, E_a, can be calculated by performing a linear fit of ln k versus $1/T$, as shown in Fig. 10. The activation energy was found to be 34.4 kJ mol^{-1} and k_o was 2.304 min^{-1}. These results are in line with those published by other authors (see Table 1), corresponding to characteristic values of complete phenol oxidation, and not to recombination or polymerization reactions to form tars, which are common when the experiments take place without controlled oxygen excess.

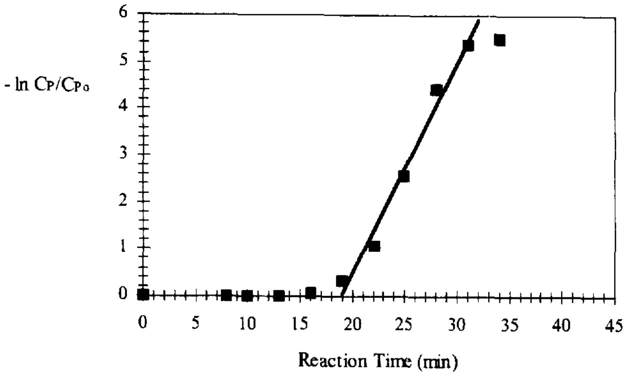

Fig. 9. Linear fit of fast reaction phase experimental data from run 5.

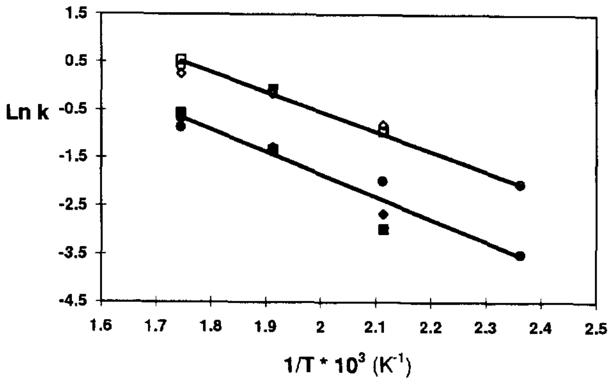

Fig. 10. Pseudo-first-order rate constants for phenol wet oxidation versus $1/T$. Empty symbols correspond to phenol concentration results and filled symbols are for COD results. ◆ and ◇, 100 bar; ● and ○, 150 bar; ■ and □, 200 bar.

Similar kinetic analysis can be done based on COD experimental data, obtaining an activation energy of 38.6 kJ mol^{-1} and a k_o value of 1707 min^{-1}. As was expected, this activation energy is slightly higher than that obtained from phenol disappearance, since COD removal depends on intermediate product oxidation, like simple organic acids, which present great resistance to oxidation.

3.2. Induction time versus temperature and pressure

The induction time (t_I) is strongly dependent on temperature (see Figs. 3–8), and it is also affected by pressure. Experimental results of induction time for several pressures and temperatures are presented in Table 3. A non-linear fit of these times has been proved to an Arrhenius-type equation that includes a pressure term (Eq. (3)), obtaining a correlation coefficient of 0.999.

$$t_I = \frac{k_I}{P} e^{E_I/RT} \tag{3}$$

Table 3
Experimental induction times for several operating conditions

	Induction time (min)			
	150 °C	200 °C	250 °C	300 °C
100 bar	> time ran	18.9	3.1	0.4
150 bar	184	15.3	1.1	0.1
200 bar	> time ran	12.6	0.9	0

where E_I is the activation energy for the induction period, k_I a pre-exponential constant and P the reaction pressure.

An E_I value of 84.842 kJ mol^{-1} and a k_I value of 9.1868×10^{-7} bar min were found. This E_I value, as it is theoretically expected, is much greater than that of the fast reaction phase, since in the induction phase the reaction is very slow and induction time is markedly affected by reaction temperature.

On the other hand, Eq. (3) is consistent with results obtained by other authors [13,14], who determined pseudo-first-order kinetics for the induction period. Thus, a similar expression to Eq. (2) can be used to obtain the induction time:

$$\begin{aligned} t_I &= -\frac{1}{k_I}\ln\frac{C_P}{C_{Po}} \\ &= -\frac{1}{k_0\,e^{-E_I/RT}}\ln\frac{C_P}{C_{Po}} \\ &= -\frac{\ln(C/C_{Po})}{k_0}\,e^{E_I/RT} \end{aligned} \tag{4}$$

In this way, it is possible to identify both pre-exponential terms from Eqs. (3) and (4)

$$\frac{k_I}{P} = -\frac{\ln(C/C_{Po})}{k_0} \tag{5}$$

This result shows that k_0 (pre-exponential factor corresponding to the induction period) is a reaction-pressure function. Since reaction initiators are formed during the induction period, it can be supposed that a pressure increase favours the formation of initiators.

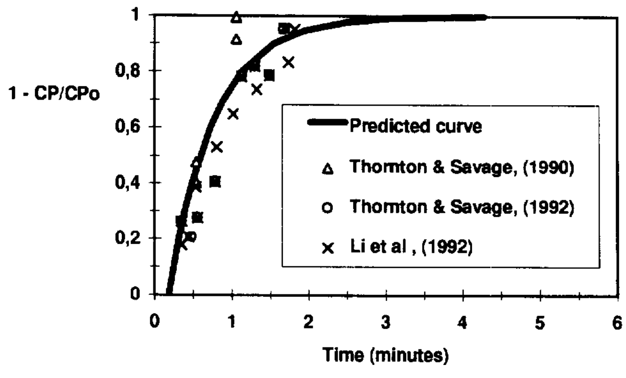

Fig. 11. Comparison of predicted elimination efficiency versus time for 280 bar and 300 °C (———) to published data: Δ, Thornton and Savage (1990); ○, Thornton and Savage (1992); ×, Li et al. (1992).

Once the kinetic equation has been parametrized, and induction time dependence on pressure and temperature has been modelized, it is possible to predict experimental results from phenol wet air oxidation experiments (Figs. 3–8). Furthermore, the integrated kinetic equation parametrized at phenol concentration units (Eq. (6)) has been used to fit published experimental data obtained using a tubular flow reactor [19,20,22] in which phenol wet oxidation took place at 300 °C and 280 bar. Fig. 11 shows a very good agreement despite the fact that published data presented great dispersion due to different oxygen excess percentages.

$$\ln\frac{C_P}{C_{Po}} = 2.304\,e^{-34.400/RT}\left[t - \frac{9.1868\times10^{-7}}{P}\,e^{84.842/RT}\right] \tag{6}$$

4. Conclusions

A kinetic equation is put forward for phenol wet air oxidation, covering the entire range of temperatures (150–300 °C) and pressures (100–200 bar). This equation has a term for the induction period and another for the oxidation phase. The oxidation term is only temperature dependent but the induction period is pressure and temperature dependent. Both terms are Arrhenius-type temperature dependent.

The integrated form of the proposed pseudo-first-order kinetic equation is:

$$\ln\frac{C_P}{C_{Po}} = k(t - t_I)$$

where

$$k = k_o\,e^{-E_R/RT}$$

and

$$t_I = \frac{k_I}{P}\,e^{E_I/RT}$$

The values of all kinetic parameters were found as follows:

$E_a = 34.4$ kJ mol^{-1} $E_I = 84.842$ kJ mol^{-1}

$k_o = 2.304$ min^{-1} $k_I = 9.1868\times10^{-7}$ bar min

After parametrization, the proposed kinetic model accurately fits the performance of phenol wet air oxidation process.

References

[1] J.A. García-Portilla, F.V. Diez, J. Coca, Métodos alternativos para el tratamiento de Efluentes Fenólicos Industriales. Ing. Quím. 238 (1989) 151–158.

[2] U.S. Kulkarni, S.G. Dixit, Destruction of phenol by oxidation with SO_3^{2-}–O_2, Ind. Eng. Chem. Res. 30 (1991) 1916–1920.

[3] F.J. Zimmerman, New waste disposal process, Chem. Eng. (1958) 117–120.

[4] F.J. Zimmerman, D.G. Diddams, The Zimmerman process and its aplication to the pulp and paper industry, Tappi 43 (1960) 710.

[5] M.A.G. Vorstman, M. Tels, Wet air oxidation of toxic wastewater, in K.J.A. De Wall, W.J. Van Der Brink (Eds.), Environ. Technol., Proc. Eur. Conf., 2nd, Nijhoff, 1987, pp. 247–55.

[6] C.R. Baillod, R.A. Lamporter, B.A. Barna, Wet oxidation for industrial waste treatment, Chem. Eng. Progress 3 (1985) 52–55.

[7] M.J. Dietrich, T.L. Randall, P.J. Canney, Wet air oxidation of hazardous organics in wastewater, Environ. Progr. 4 (3) (1985) 171–177.

[8] J.N. Foussard, H. Debellefontaine, J. Besombes-Vailhé, Efficient elimination of organic liquid wastes wet air oxidation, J. Environ. Eng. 115(2) (1989) 367–385.

[9] L.V. Shibaeva, D.I. Metelitsa, E.T. Denisov, Oxidation of phenol with molecular oxygen in aqueous solutions, Kin. Car. 10 (5) (1969) 832.

[10] A. Sadana, Ph.D. Thesis, University of Delaware, 1976.

[11] B.B. Pruden, H. Le, Wet air oxidation of soluble components in waste water, Can. J. Chem. Eng. 54 (1976) 319.

[12] R.K., Helling, M.K. Strobel, R.J. Torres, report OR NL/MIT-332, Oak Ridge National Laboratory, 1981.

[13] R.S. Willms, D.D. Reible, D.M. Wetzel, D.P. Harrison, Aqueous-phase oxidation: rate enhancement studies, Ind. Eng. Chem. Res. 26 (1987) 606–612.

[14] H. Joglekar, S.D. Samant, J.B. Joshi, Kinetics of wet air oxidation of phenol and substituted phenols, Water Res. 25(2) (1991) 135–145.

[15] R.S. Willms, A.M. Balinsky, D.D. Reible, D.M. Wetzel, D.P. Harrison, Analysis of high pressure, multiphase, batch reactor data, Environ. Progr. 4(2) (1985) 131–135.

[16] H.R. Devlin, I.J. Harris, Mechanism of the oxidation of aqueous phenol with dissolved oxygen, Ind. Eng. Chem. Fundam. 23 (1984) 387–392.

[17] L.S. Clesceri, A.E. Greenberg, R.R. Trussell (eds.), APHA AWWA WPCF. Standard Methods. For the Examination of Water and Wastewater, 17th edn., 1989.

[18] C. Collivignarelli, G. Bissolotti, Esperienze nel trattamento di reflui mediante ossidazione a umido: fattibilità tecnico-economica, Ing. Ambientale 17(10) (1988) 542–553.

[19] T.D. Thornton, P.E. Savage, Phenol oxidation in supercritical water, J. Supercritical Fluids 3 (1990) 240–8.

[20] T.D. Thornton, P.E. Savage, Kinetics of phenol oxidation in supercritical water, AIChe J. 32(3) (1992) 321–27.

[21] T.D. Thornton, P.E. Savage, Phenol oxidation pathways in supercritical water, Ind. Eng. Chem. Res. 31(11) (1992) 2451–2456.

[22] R. Li, T.D. Thornton, P.E. Savage, Kinetics of CO_2 formation from the oxidation of phenols in supercritical water, Environ. Sci. Technol. 26 (1992) 2388–2395.

[23] O. Levenspiel, Chemical Reaction Engineering, Wiley, New York, 2nd edn.